

# Experimental evidence of logarithmic relaxation in single-particle dynamics of hydrated protein molecules

Xiang-qiang Chu,<sup>a</sup> Marco Lagi,<sup>ab</sup> Eugene Mamontov,<sup>c</sup> Emiliano Fratini,<sup>b</sup> Piero Baglioni<sup>b</sup> and Sow-Hsin Chen<sup>\*aa</sup>

Received 8th February 2010, Accepted 27th April 2010

First published as an Advance Article on the web 24th May 2010

DOI: 10.1039/c002602f

**We observe a logarithmic-like decay of the intermediate scattering function (ISF) of the hydrogen atoms in the protein molecule in the time interval from 10 ps to 1 ns. We analyze the ISF,  $F_H(Q,t)$ , in terms of an asymptotic expression proposed by mode coupling theory (MCT). The result clearly shows that this logarithmic stretching of the  $\beta$ -relaxation range is real, substantiating the prediction of the molecular dynamics (MD) simulation results that used the formula proposed by MCT for the analysis of ISF.**

Globular proteins are hetero-polymers consisting of densely packed amino acid chains. Although crystallographic structures are known for many of them, these static structures alone are not sufficient to understand their biological behavior. Their function is in fact eventually governed by their slow conformational dynamics.<sup>1,2</sup> Protein dynamics, triggered by thermal energy ( $k_B T$  per atom), allows the biomolecule to sample many conformations around the average structure, the so-called conformational substates (CSs). A complete description of proteins requires therefore a multidimensional potential energy landscape (EL), a concept proposed for proteins by Frauenfelder and co-workers in the 1970s.<sup>3-5</sup> The EL defines the relative probabilities of the CS (the minima) and the energy barriers between them (the maxima). In particular, the EL of a complex system that contains  $N$  atoms is described by the potential energy surface in a space of  $3N$  dimensions, where each axis gives one coordinate of a specific atom.

As a first approximation, protein dynamics can be divided into two main groups according to their timescale or, equivalently, to the region of the EL sampled.<sup>1</sup> (a) Slow timescale dynamics ( $\mu$ s to ms, or the  $\alpha$ -relaxation) define fluctuations between states separated by energy barriers of  $E_A \gg k_B T$ , *i.e.* large-amplitude collective motions. Biological processes like enzyme catalysis and protein–protein interactions occur on this timescale. (b) Fast timescale dynamics (1 ps to 10 ns, or  $\beta$ -relaxation) define fluctuations between structurally similar states that are separated by  $E_A < k_B T$ . They are more local, small-amplitude fluctuations at physiological temperature like loop motions and side-chain rotations.

Slow and fast dynamics are somehow linked to each other. The correlation between dynamics and biological activity has been demonstrated on the  $\mu$ s to ms timescale, but fluctuations at atomic level are much faster than this, leading to the more complex idea of

a hierarchy of substates.<sup>3-5</sup> The EL is organized in a fractal-like hierarchy of a number of tiers; there are valleys within valleys. Some aspects of protein dynamics are also ‘slaved’ to the solvent fluctuations, with the protein component dictating the relative rates.<sup>6,7</sup>

Molecular dynamics (MD) simulations have the advantage that they can describe protein dynamics completely: the position of each atom can be followed any instant in time, so they are the ideal tool to study ps to ns (fast) protein dynamics.

By means of MD, we showed in a previous paper<sup>8</sup> how the fast dynamics of hydrated lysozyme powder follows a logarithmic relaxation in the time domain. In particular, we were able to fit the protein single-particle intermediate scattering function between 2 ps and 5 ns with the predictions of the mode coupling theory (MCT) for systems close to a high-order singularity. So the relaxation dynamics of globular proteins may also be described by the MCT.<sup>9</sup>

The fact that the most popular glass transition theory, *i.e.* the MCT,<sup>10</sup> can be used to explain glassy dynamics of proteins should not be surprising. It is well-known, in fact, that the dynamics of native globular proteins has much in common with the dynamics of glass-forming liquids.<sup>11-17</sup> They both consist of non-crystalline packing in which their constituents (molecules or amino acid residues) assemble. They also have a complex EL, composed of a large number of alternative conformations at similar energies.<sup>11</sup> Other similarities are the so-called glass transition<sup>12,13</sup> (sudden change of slope in their hydrogen atoms mean square displacement as a function of  $T$ ), the boson peak<sup>14</sup> (typical of strong glass formers), and the two types of equilibrium fluctuations, the cooperative  $\alpha$  (involving large domains of the biomolecule) and the local  $\beta$  (involving side-chains), typical of glass-formers.<sup>16</sup>

Proteins and glasses are stochastic complex systems, and one of the distinctive features of complex systems is a slow non-exponential relaxation of the density and single-particle correlation functions  $\phi_q(t)$  observed in a wide range of timescales. The time dependence of the relaxation scenario usually follows these three steps: it begins with (a) a short-time Gaussian-like ballistic region, followed by (b) the  $\beta$ -relaxation region which is governed by either two power-law decays  $\phi_q(t) \approx (t/\tau_q^\beta)^{-a}$  and  $\phi_q(t) \approx (-t/\tau_q^\beta)^b$  or a logarithmic decay  $\phi_q(t) \approx A_q - B_q \ln(t/\tau^\beta)$ , which then evolves into (c) an  $\alpha$ -relaxation region that is governed by a stretched exponential decay (or Kohlrausch–Williams–Watts law),  $\phi_q(t) \approx \exp(-t/\tau_q^\alpha)^\beta$ . These types of relaxation are characteristic of complex systems,<sup>18</sup> just as the simple exponential relaxation (or Debye law)  $\phi_q(t) \approx \exp(-t/\tau_q)$  is typical for gases and liquids. Proteins and glasses have also important differences: both systems are aperiodic, but the organization of protein EL is far more sophisticated than the glass one.

It is in principle possible to study the relaxation dynamics of protein in the time range of several picoseconds to several

<sup>a</sup>Department of Nuclear Science and Engineering, Massachusetts Institute of Technology, Cambridge, MA, 02139, USA. E-mail: sowhsin@mit.edu

<sup>b</sup>Department of Chemistry and CSGI, University of Florence, Sesto Fiorentino, Florence, I-50019, Italy

<sup>c</sup>Spallation Neutron Source, Oak Ridge National Laboratory, Oak Ridge, TN, 37831, USA

nanoseconds through the measurement of the intermediate scattering function (ISF)  $F_H(Q,t)$ , which is equivalent to the  $\phi_q(t)$  in the theory, with new generation of backscattering instruments.<sup>19</sup> In this communication, we perform two separate experiments on two different backscattering instruments<sup>19,20</sup> and demonstrate the possibility of studying the protein dynamics in the  $\beta$ -relaxation region by both spectrometers. After thoroughly correcting for the background from the experimental data signal, we first show the logarithmic-like decay in the ISF in time domain obtained from Fourier transformation of the background corrected quasi-elastic neutron scattering (QENS) spectra. We then analyze the ISF by the asymptotic formula developed by MCT and compare the fitting parameters in both experiments. It is striking that the two separate experiments involving two batches of samples give consistent sets of results, supporting the logarithmic relaxation scenario.

We use D<sub>2</sub>O hydrated protein sample in order to obtain signals which is dominated by contribution of the incoherent scattering from hydrogen atoms of the protein molecules. In this study we choose hen egg white lysozyme (L7651, three times crystallized, dialysed and lyophilized) which has a molecular weight of 14.4 kDa. The protein powder, as was purchased from Fluka, was used without further purification, except an extensive lyophilization to remove any water left. The dried protein powder was then hydrated isopiesticly at 5 °C by exposing it to D<sub>2</sub>O vapor in a closed chamber (RH = 100%) until  $h = 0.34$  is reached (*i.e.* 0.34 g D<sub>2</sub>O per g dry lysozyme). The hydration level was determined by thermo-gravimetric analysis and also confirmed by directly measuring the weight of absorbed D<sub>2</sub>O. This hydration level was chosen to have almost a monolayer of heavy water covering the protein surface.<sup>21</sup> Differential scanning calorimetry (DSC) analysis was performed in order to detect the absence of any feature that could be associated with the presence of bulk-like water.

Two separate experiments were performed using two backscattering spectrometers with different resolutions and dynamic ranges, in order to be able to obtain the broad range of relaxation time from 10 ps to 1 ns. One is a near-backscattering spectrometer BASIS at the Spallation Neutron Source (SNS) in Oak Ridge National Laboratory (ORNL), and the other is the High-Flux Backscattering Spectrometer (HFBS) in NIST Center for Neutron Research (NCNR). For the chosen experimental setup, the BASIS has an energy resolution of 3.4  $\mu$ eV (full-width at half-maximum, for the  $Q$ -averaged resolution value) and a dynamic range of  $\pm 100$   $\mu$ eV; the HFBS spectrometer has an energy resolution of 0.8  $\mu$ eV (full width at half-maximum) and a dynamic range of  $\pm 36$   $\mu$ eV.<sup>20</sup>

The QENS measurement essentially gives the self-dynamic structure factor  $S_H(Q,\omega)$  of the hydrogen atom in a typical protein molecule convolved with the energy resolution function  $R(Q,\omega)$  of the instrument. The  $S_H(Q,\omega)$  can be presented as the Fourier transform of the ISF  $F_H(Q,t)$  of the hydrogen atom of the protein molecule, *i.e.*,

$$S_H(Q,\omega) = FT[F_H(Q,t) R(Q,t)], \quad (1)$$

Then the ISF  $F_H(Q,t)$  can be easily calculated by dividing the Fourier transform of the measured data (after subtracting the background)  $F_m(Q,t) = FT[S_H(Q,\omega)]$ , with the Fourier transform of the resolution function  $R(Q,t)$ :

$$F_H(Q,t) = F_m(Q,t)/R(Q,t) \quad (2)$$

In this communication, we use an asymptotic expression derived from mode coupling theory (MCT) to fit the ISF  $F_H(Q,t)$ :<sup>22,23</sup>

$$F_H(Q,t) \approx [f(Q,T) - H_1(Q,T)\ln(t/\tau_\beta(T)) + H_2(Q,T)\ln^2(t/\tau_\beta(T))]\exp(t/\tau_\alpha(Q,T)) \quad (3)$$

where  $\tau_\beta(T)$  and  $\tau_\alpha(Q,T)$  are the characteristic  $\beta$ - and  $\alpha$ -relaxation time respectively, and  $f(Q,T)$  is the  $Q$ -dependent prefactor which can be written as a function of temperature, proportional to the Debye-Waller factor for small  $Q$ ,  $f(Q,T) = \exp[-A(T)Q^2]$ . The parameters  $H_1(Q,T)$  and  $H_2(Q,T)$  can be written as  $H_1(Q,T) = h_1(Q)B_1(T)$  and  $H_2(Q,T) = h_1(Q)B_2(Q,T)$ , where the  $Q$  dependence of  $h_1(Q)$  is a power law of  $Q$  for small  $Q$ ,<sup>8</sup> and the temperature dependent factor  $B_1(T)$  goes like  $|T/T_C - 1|^{1/2}$ , where  $T_C$  is the MCT critical temperature.<sup>23</sup>

Since our experimental measured time range (10 ps to 1 ns) is much shorter than the  $\alpha$ -relaxation time range, *i.e.*,  $t$  is much smaller than  $\tau_\alpha$ , we can simply put the last exponential factor to be unity and fit the measured ISF with a simpler expression:

$$F_H(Q,t) \approx [f(Q,T) - H_1(Q,T)\ln(t/\tau_\beta(T)) + H_2(Q,T)\ln^2(t/\tau_\beta(T))] \quad (4)$$

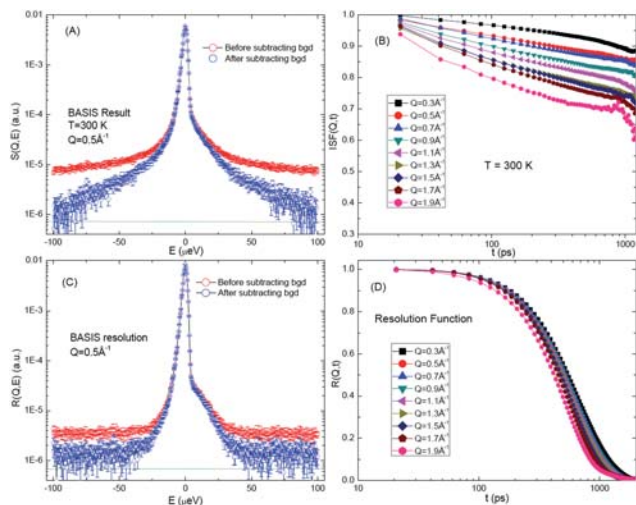
Before Fourier-transformation of the BASIS data from the energy into the time domain, we have carefully subtracted background from the experimental spectra. Failure to perform proper background subtraction would not significantly affect the so-obtained ISF at long times, but would distort its behavior around  $t \approx 0$  due to termination error of the Fourier transformation. On the BASIS, as well as on any other neutron spectrometer, the measured background includes sample-independent and sample- (and temperature) dependent contributions. While the former is easy to subtract explicitly using the calibration measurements of the empty sample holder, empty sample environment equipment, *etc.*, the latter has to be evaluated. In the past, it has been assumed that the sample-dependent background is approximately constant as a function of the experimentally measured neutron time-of-flight (TOF). In the energy space, this would yield a background term non-linear in the energy transfer. Indeed, we have found that such a non-linear background adequately describes the background in the data fits. In this work, we have taken a further step in the background evaluation as follows. Since the background signal was found to be proportional to the incident flux of the sample, in the course of the data reduction we subtracted from the raw data (in TOF, or incident wavelength) not merely a constant, but rather the incident beam spectrum measured at the incident beam monitor and properly offset in the TOF to account for the distances between the monitor, sample, crystal analyzers and neutron detectors. Since the incident intensity on the BASIS is somewhat wavelength-dependent, this approach to background subtraction is more accurate than simply subtracting a constant in the TOF raw data assuming a wavelength-independent background. Thus, the spectral shape of the background to be subtracted from the raw data is determined from the monitor data. The amount of the background to be subtracted is determined in the course of iterative procedure, where progressively larger background spectrum (of the fixed spectral shape) is subtracted from the raw data presented as a function of the incident wavelength until the resulting spectrum in the energy transfer satisfies the temperature-dependent detailed balance condition,  $S(Q,\omega) = \exp(E/k_B T)S(Q,-\omega)$ . Here  $k_B$  is the Boltzmann constant,  $E$  is the energy transfer, and  $Q$  is the scattering momentum transfer.

Even after evaluation and subtraction of the background, the  $S_H(Q, \omega)$  spectra do not necessarily decay to near-zero values at the extremes of the measured energy transfer. This is because of the possible presence of the relaxation processes that are not instrument background artifacts, but are simply too fast for the dynamic range of the experiment. Therefore, prior to Fourier-transformation, we have subtracted a constant from the  $S_H(Q, \omega)$  spectra already corrected for the background to suppress the termination error. The resulting  $F_H(Q, t)$  spectra represent the ISF that describes the processes reliably measurable in the dynamic range of the experiment.

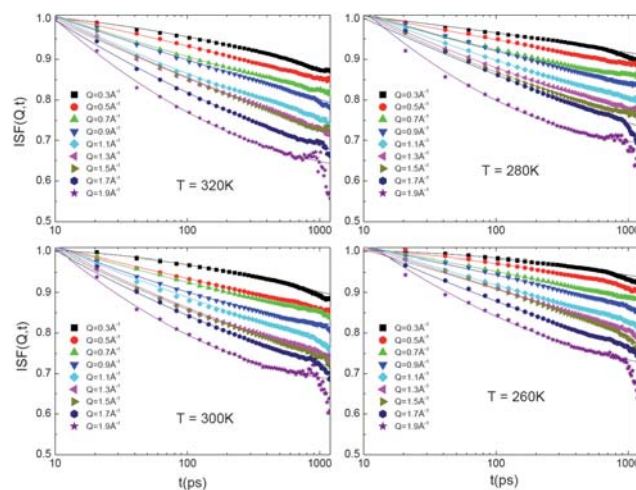
For the QENS data obtained from HFBS, the Fourier transformation and the deconvolution procedures were performed using the FFT toolkit in DAVE software package developed by NCCR.<sup>24</sup>

Fig. 1 shows the above subtraction and deconvolution procedures in details. Panels (A) and (C) show the QENS spectra taken at 300 K and resolution at 10 K at a specific  $Q = 0.5 \text{ \AA}^{-1}$  respectively. The figures are plotted on a log scale to show the difference of the data before and after background subtraction. A small value of constant background (shown in the figure by the green dotted lines) was also subtracted before Fourier transformation. All the QENS spectra were normalized before applying Fourier transformation and deconvolution procedures. Panel (D) shows the Fourier transforms of the resolution function  $R(Q, t)$  at nine different  $Q$  values. Panel (B) shows the result of dividing the Fourier transformed data with  $R(Q, t)$  (as shown by eqn (2)) at the above nine different  $Q$  values at 300 K. From these ISFs we can see that the measurement timescale is approximately 10 ps to 1 ns, which is within the  $\beta$ -relaxation range of the protein.

In Fig. 2 and 3, we fit the ISF  $F_H(Q, t)$  calculated from the analysis of QENS spectra taken from BASIS and HFBS respectively, according to eqn (4). We essentially use four parameters,  $A(T)$ ,  $\tau_\beta(T)$ ,  $H_1(Q, T)$  and  $H_2(Q, T)$ . While  $A(T)$  and  $\tau_\beta(T)$  are  $Q$ -independent and  $A(T)$  represents the prefactor  $f(Q, T)$  by the relation of the Debye-Waller factor. We analyze the curves at all nine  $Q$ -values together to



**Fig. 1** (A) Normalized QENS spectra at  $T = 300 \text{ K}$  and  $Q = 0.5 \text{ \AA}^{-1}$ , before (red circle) and after (blue circle) background subtraction. (B) Intermediate scattering function (ISF) of the QENS spectra at nine different  $Q$  values. (C) Resolution spectra taken at  $Q = 0.5 \text{ \AA}^{-1}$ , before and after background subtraction. (D) Fourier transforms of the BASIS resolution functions at nine different  $Q$  values.



**Fig. 2** Analysis of the  $\beta$ -relaxation range of the ISF according to eqn (4). The ISF is calculated from the analysis of QENS spectra taken from BASIS at four different temperatures  $T = 320 \text{ K}$ ,  $300 \text{ K}$ ,  $280 \text{ K}$  and  $260 \text{ K}$ , at nine  $Q$  values.

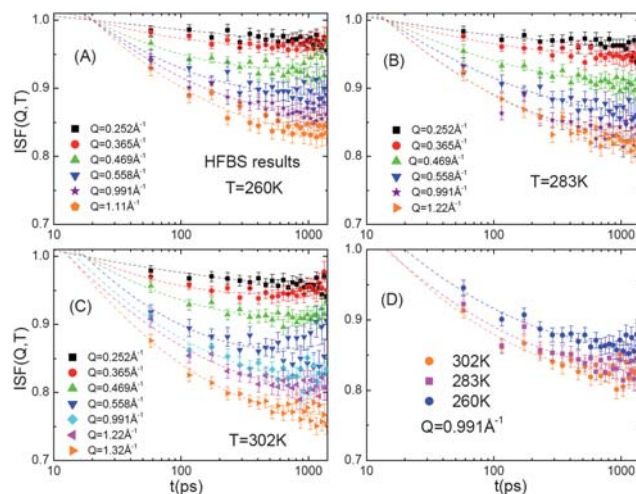


**Fig. 3** Analysis of the ISF calculated from QENS spectra taken from HFBS at three different temperatures  $T = 302 \text{ K}$ ,  $283 \text{ K}$  and  $260 \text{ K}$ , at different  $Q$  values. Panel (D) represents the comparison of the ISF at three temperatures at the same  $Q$  value.

obtain the  $Q$ -independent parameters as well as the  $Q$ -dependent parameters. The fitting results show that all the  $F_H(Q, t)$  values at all nine  $Q$ s merge to a value  $f(Q, T)$  which is very close to 1 at a specific short time ( $\tau_\beta(T)$ , usually around 10 ps). It does not directly go to 1 since our measured time range is not short enough for us to tell what happens in the time range less than 10 ps. Note that there is an upturn in the data in large  $Q$  region in Fig. 2 and 3 and a downturn in the data in small  $Q$  region in Fig. 2. This is due to the presence of the second order term  $H_2(Q, T) \ln^2(t/\tau_\beta(T))$  which gives the positive or negative curvatures to the otherwise straight line. We thus obtain the values of  $H_1(Q, T)$  and  $H_2(Q, T)$  by fitting the curves in the measured time range.

Fig. 4 shows the  $Q$  dependence of the fitting parameters obtained from both BASIS and HFBS. We find that  $H_1(Q, T)$  obeys a power law in  $Q$  at small  $Q$ , i.e.  $H_1(Q, T) = B_1(T)Q^\beta$ , where the power  $\beta$  is

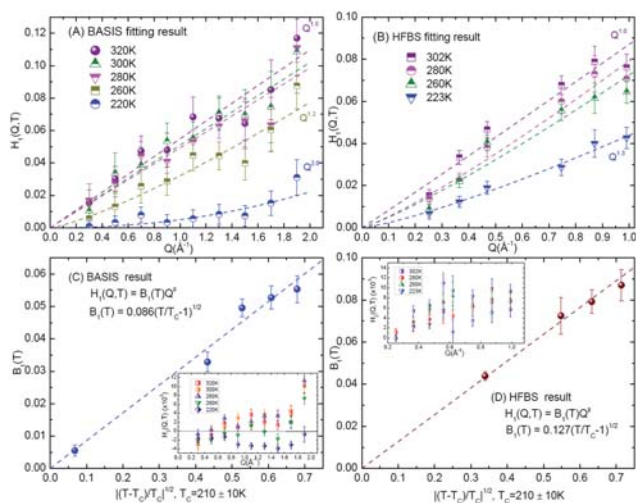


**Fig. 4** Analysis of the fitting results from both BASIS (panels (A) and (C)) and HFBS (panels (B) and (D)) instruments. Panels (A) and (B) show the fitted  $H_1(Q, T)$  values as a function of  $Q$  for both cases at different temperatures, which is found to obey a power law of  $Q$ , *i.e.*  $H_1(Q, T) = B_1(T)Q^\beta$ . Panels (C) and (D) show the fitted  $B_1(T)$  values plotted as a function of  $|(T - T_C)/T_C|^{1/2}$ , where  $T_C$  is the critical MCT temperature and is chosen to make  $B_1(T)$  linearly dependent on  $|(T - T_C)/T_C|^{1/2}$ . The inset of panels (C) and (D) show the fitted  $H_2(Q, T)$  values as a function of  $Q$  for BASIS and HFBS respectively.

a value between 1 and 2,  $B_1(T)$  is a temperature dependent parameter. We then plot the fitted  $B_1(T)$  values as a function of  $|(T - T_C)/T_C|^{1/2}$ , where  $T_C$  is the MCT critical temperature and is chosen to make  $B_1(T)$  linearly dependent on  $|(T - T_C)/T_C|^{1/2}$ . We found that  $T_C$  is about  $210 \pm 10$  K, and is consistent in both experiments. This value is also very close to the well-known dynamic transition temperature in protein  $T_D \approx 220$  K.<sup>12,13,25,26</sup>

Previous analyses<sup>27</sup> on QENS data obtained from proteins simply fit the data with a single Kohlrausch–Williams–Watts (KWW) stretched exponential function, which simplifies the protein relaxation process to only the  $\alpha$ -relaxation. However, while in the QENS measurement range proteins cannot relax completely, our analysis provides a reasonable way of approaching the  $\beta$ -relaxation process. We demonstrated in the above analysis that the logarithmic stretching of the  $\beta$ -relaxation range is consistent with that predicted by the MD simulation,<sup>8</sup> although we would not preclude different scenarios proposed by other researchers<sup>16,28,29</sup> due to the large error bars in our measured ISF.

Recent neutron scattering experiments<sup>30</sup> and MD simulations<sup>31</sup> have demonstrated that the rotational and reorientational dynamics of methyl groups are the processes associated with the  $\beta$ -relaxations and these  $\beta$ -relaxation processes are solvent-independent. However, our measured decay time in the  $\beta$ -relaxation range is both  $Q$  and  $T$  dependent, indicating that the logarithmic-like relaxation process can include processes other than the methyl group rotations. On the other hand, a unified model of protein dynamics has been recently proposed by H. Frauenfelder and collaborators,<sup>16</sup> which implies that the fluctuations in the hydration water molecules also control protein internal motions. This scenario provides a possible way to explain the origin of the relaxation process we observe here. It contains both solvent-independent  $\beta$ -relaxation introduced by the rotational dynamics of methyl groups and the solvent-induced relaxation. Also

in our previous experiments,<sup>32,33</sup> we observe a dynamic crossover temperature  $T_L \approx 220$  K in the protein hydration water, which is very close to the critical temperature  $T_C$  shown in Fig. 4. This result provides another evidence that the intermediate time motion of proteins is partly controlled by the hydration water.<sup>7</sup>

In summary, while the  $\alpha$ -relaxation time in globular protein like lysozyme is too long for the present day QENS study (in the 1  $\mu$ s to 1 ms range), the state-of-the-art backscattering instrument such as BASIS and HFBS is capable of studying the  $\beta$ -relaxation range (*i.e.* 10 ps to 10 ns range) effectively. Using the asymptotic formula derived from the MCT, we are able to demonstrate that the well-known dynamic transition temperature  $T_D$  of lysozyme can be identified as a critical temperature  $T_C$  of the MCT. If we interpret the  $T_C$  as the crossover temperature  $T_X$  implied by the extended mode coupling theory (eMCT),<sup>34,35</sup> the well-known dynamic transition temperature at about 220 K<sup>12,13,25,26</sup> (or sometimes called the glass transition temperature) can be understood as the eMCT crossover temperature.

## Acknowledgements

The research at MIT is supported by DOE Grants No. DE-FG02-90ER45429. This work utilized facilities supported in part by the National Science Foundation under Agreement No. DMR-0086210. We appreciate technical supports during experiments from M. Tyagi, and A. Faraone of NIST Center for Neutron Research. EF and PB acknowledge financial support from CSGI and MIUR. The neutron scattering experiment at Oak Ridge National Laboratory's Spallation Neutron Source was sponsored by the Scientific User Facilities Division, Office of Basic Energy Sciences, US Department of Energy.

## References

- 1 K. A. Henzler-Wildman, M. Lei, V. Thai, S. J. Kerns, M. Karplus and D. Kern, *Nature*, 2007, **450**, 913–916.
- 2 K. Henzler-Wildman and D. Kern, *Nature*, 2007, **450**, 964–972.
- 3 R. H. Austin, K. W. Beeson, L. Eisenstein, H. Frauenfelder and I. C. Gunsalus, *Biochemistry*, 1975, **14**, 5355–5373.
- 4 H. Frauenfelder, S. G. Sligar and P. G. Wolynes, *Science*, 1991, **254**, 1598–1603.
- 5 J. N. Onuchic, Z. Luthey-Schulten and P. G. Wolynes, *Annu. Rev. Phys. Chem.*, 1997, **48**, 545–600.
- 6 D. Vitkup, D. Ringe, G. A. Petsko and M. Karplus, *Nat. Struct. Biol.*, 2000, **7**, 34–38.
- 7 P. W. Fenimore, H. Frauenfelder, B. H. McMahon and F. G. Parak, *Proc. Natl. Acad. Sci. U. S. A.*, 2002, **99**, 16047–16051.
- 8 M. Lagi, P. Baglioni and S. H. Chen, *Phys. Rev. Lett.*, 2009, **103**, 108102.
- 9 W. Doster, S. Cusack and W. Petry, *Phys. Rev. Lett.*, 1990, **65**, 1080–1083.
- 10 W. Gotze and L. Sjogren, *Rep. Prog. Phys.*, 1992, **55**, 241–376.
- 11 C. A. Angell, *Science*, 1995, **267**, 1924–1935.
- 12 W. Doster, S. Cusack and W. Petry, *Nature*, 1989, **337**, 754–756.
- 13 B. F. Rasmussen, A. M. Stock, D. Ringe and G. A. Petsko, *Nature*, 1992, **357**, 423–424.
- 14 H. Leyer, W. Doster and M. Diehl, *Phys. Rev. Lett.*, 1999, **82**, 2987–2990.
- 15 J. L. Green, J. Fan and C. A. Angell, *J. Phys. Chem.*, 1994, **98**, 13780–13790.
- 16 H. Frauenfelder, G. Chen, J. Berendzen, P. W. Fenimore, H. Jansson, B. H. McMahon, I. R. Stroe, J. Swenson and R. D. Young, *Proc. Natl. Acad. Sci. U. S. A.*, 2009, **106**, 5129–5134.
- 17 P. Etchegoin, *Phys. Rev. E: Stat. Phys., Plasmas, Fluids, Relat. Interdiscip. Top.*, 1998, **58**, 845–848.
- 18 V. A. Avetisov, A. K. Bikulov and V. Al Osipov, *J. Phys. A: Math. Gen.*, 2003, **36**, 4239–4246.

- 19 E. Mamontov, M. Zamponi, S. Hammons, W. S. Keener, M. Hagen and K. W. Herwig, *Neutron News*, 2008, **19**, 22–24.
- 20 A. Meyer, R. M. Dimeo, P. M. Gehring and D. A. Neumann, *Rev. Sci. Instrum.*, 2003, **74**, 2759–2777.
- 21 G. Careri, *Prog. Biophys. Mol. Biol.*, 1998, **70**, 223–249.
- 22 F. Sciortino, P. Tartaglia and E. Zaccarelli, *Phys. Rev. Lett.*, 2003, **91**, 268301.
- 23 W. Gotze and M. Sperl, *Phys. Rev. E: Stat., Nonlinear, Soft Matter Phys.*, 2002, **66**, 011405.
- 24 R. T. Azuah, L. R. Kneller, Y. Qiu, P. L. W. Tregenna-Piggott, C. M. Brown, J. R. D. Copley and R. M. Dimeo, *J. Res. Natl. Inst. Stand. Technol.*, 2009, **114**, 341–358.
- 25 G. Zaccai, *Science*, 2000, **288**, 1604–1607.
- 26 P. W. Fenimore, H. Frauenfelder, B. H. McMahon and R. D. Young, *Proc. Natl. Acad. Sci. U. S. A.*, 2004, **101**, 14408–14413.
- 27 H. Jansson, F. Kargl, F. Fernandez-Alonso and J. Swenson, *J. Chem. Phys.*, 2009, **130**, 205101.
- 28 G. Chen, P. W. Fenimore, H. Frauenfelder, F. Mezei, J. Swenson and R. D. Young, *Philos. Mag.*, 2008, **88**, 3877–3883.
- 29 M. S. Appavou, G. Gibrat and M. C. Bellissent-Funel, *Biochim. Biophys. Acta, Proteins Proteomics*, 2009, **1794**, 1398–1406.
- 30 J. H. Roh, V. N. Novikov, R. B. Gregory, J. E. Curtis, Z. Chowdhuri and A. P. Sokolov, *Phys. Rev. Lett.*, 2005, **95**, 038101.
- 31 M. Krishnan, V. Kurkal-Siebert and J. C. Smith, *J. Phys. Chem. B*, 2008, **112**, 5522–5533.
- 32 S. H. Chen, L. Liu, E. Fratini, P. Baglioni, A. Faraone and E. Mamontov, *Proc. Natl. Acad. Sci. U. S. A.*, 2006, **103**, 9012–9016.
- 33 X. Q. Chu, A. Faraone, C. Kim, E. Fratini, P. Baglioni, J. B. Leao and S. H. Chen, *J. Phys. Chem. B*, 2009, **113**, 5001–5006.
- 34 S. H. Chong, S. H. Chen and F. Mallamace, *J. Phys.: Condens. Matter*, 2009, **21**, 504101.
- 35 S.-H. Chong, *Phys. Rev. E: Stat., Nonlinear, Soft Matter Phys.*, 2008, **78**, 041501.